Journal of the Optical Society of America B
OPTICAL PHYSICS

Experimental pre-assessing of two-mode entanglement in Gaussian state mixing

Adriana Pecoraro,[1] Daniela Buono,[2] Gaetano Nocerino,[3] Alberto Porzio,[4] Stefano Olivares,[5,6] and Matteo G. A. Paris[5,6,*]

[1]Dipartimento di Scienze Fisiche, Università "Federico II," Complesso Univ. Monte Sant'Angelo, I-80126 Napoli, Italy
[2]Dipartimento di Ingegneria Industriale, Università degli Studi di Salerno, I-84084 Fisciano (SA), Italy
[3]Trenitalia spa, DPR Campania, IMC Campi Flegrei, I-80124 Napoli, Italy
[4]CNR—SPIN, Unitá di Napoli, Complesso Univ. Monte Sant'Angelo, I-80126 Napoli, Italy
[5]Quantum Technology Lab, Dipartimento di Fisica dell'Università degli Studi di Milano, I-20133 Milano, Italy
[6]Istituto Nazionale di Fisica Nucleare, Sezione di Milano, I-20133 Milano, Italy
*Corresponding author: matteo.paris@fisica.unimi.it

Received 10 November 2016; revised 18 December 2016; accepted 21 December 2016; posted 21 December 2016 (Doc. ID 280615); published 23 January 2017

We suggest and demonstrate a method to assess entanglement generation schemes based on mixing of Gaussian states at a beam splitter (BS). Our method is based on the fidelity criterion and represents a tool to analyze the effect of losses and noise before the BS in both symmetric and asymmetric channels with and without thermal effects. More generally, our scheme allows one to pre-assess entanglement resources and to optimize the design of BS-based schemes for the generation of continuous-variable entanglement.

OCIS codes: (270.6570) Squeezed states; (270.5585) Quantum information and processing; (190.4970) Parametric oscillators and amplifiers.

https://doi.org/10.1364/JOSAB.34.000404

1. INTRODUCTION

Continuous-variable (CV) entanglement is a powerful resource for optical quantum technologies, and it is the crucial ingredient for several protocols, including quantum teleportation, dense coding, and quantum-enhanced metrology. In particular, Gaussian states and Gaussian entanglement reveal themselves as the main resource in practical applications [1–9]. In fact, most CV quantum technology has been developed upon exploiting Gaussian states and Gaussian operations. In this framework, techniques for the generation, characterization, and certification of Gaussian entanglement play a crucial role and have received a large amount of attention in the last two decades.

Among the different schemes to generate CV entanglement, the mixing of Gaussian states emerged as a convenient choice, and it has been employed in several applications. In this scheme, a pair of Gaussian states is mixed at a beam splitter (BS), and entangled states are obtained at the output as far as the input signals show some nonclassical features [10–16]. Entanglement certification is usually performed *a posteriori*, by means of measurements realized at the outputs of the BS, e.g., by performing full quantum tomography of the bipartite state [17,18] or by measuring a suitable entanglement witness. On the other hand, an *a priori* certification scheme, i.e., involving measurements before the BS, would be welcome because it would permit the pre-assessing of entanglement resources and the optimization of the generation scheme, e.g., by quantum state or reservoir engineering at the input.

In this paper, we experimentally address an *a priori* certification scheme based on the fidelity criterion for entanglement generation [19]. In particular, we assess the effects of losses and noise on the generation of entanglement by Gaussian states mixing. Upon using a suitably designed experimental setup, we analyze the effect of signal propagation before the BS and evaluate threshold values on the transmission coefficient and on the thermal noise as a function of the parameter of the input signals. We consider both symmetric and asymmetric channels with and without thermal noise.

The paper is structured as follows. In Section 2 we introduce the notation and the tools to describe entanglement generation by Gaussian states mixing. We also review the fidelity criterion proposed in [19]. In Section 3 we describe Gaussian state propagation in lossy and noisy channels. In Section 4 we describe our experimental apparatus and report results for the different configurations. Section 5 closes the paper with concluding remarks.

2. FIDELITY CRITERION

As a matter of fact, there are several *a posteriori* criteria to witness entanglement of bipartite CV systems [20–24]. They may be exploited to assess whether entanglement has been produced

after a given interaction has taken place. On the other hand, an *a priori* criterion has been recently introduced [19] to assess the entanglement capability of a pair of distinct Gaussian states interacting at a BS. The criterion is based on the mutual fidelity of two uncorrelated Gaussian states, ϱ_c and ϱ_d, describing the preparation of two bosonic modes c and d, and is able to predict whether the state obtained by mixing them at a BS will be entangled or not. In more detail, this criterion states that the interaction between the two input states through a bilinear exchange Hamiltonian gives rise to entanglement if the fidelity between the two input states is less than a threshold value $F_{\rm th}$. The actual value for the threshold depends on the initial states' purities and on the beam splitter transmissivity [19], upon the assumption that no phase-shift is imposed at the BS [25].

In order to introduce the criterion, let us first review some properties of Gaussian states (GS). GS are quantum states with a Gaussian Wigner function in the phase space. Gaussian states are prominent resources in CV quantum technology because, besides being easily produced in laboratories with current technologies, they preserve their Gaussian character under linear and bilinear transformations, such as those associated with beam splitters, phase shifters, and optical amplifiers, e.g., single- and two-mode squeezing [26], as well as during propagation through a noisy channel [27]. Gaussian states are completely characterized by a finite number of parameters, e.g., by the first and second moments of quadrature mode operators. In particular, when dealing with the correlation between the two modes of a bipartite Gaussian state, one may focus only on the phase-space covariance matrix (CM) because the presence of first moments does not affect the amount of correlations.

Let us now consider the phase-space description of the two involved modes and of their dynamics. As previously mentioned, we can focus the evolution of the 4×4 CM $\Sigma_{\rm in}$ of the input states $\varrho_c \otimes \varrho_d$ (without loss of generality, we can focus on states with vanishing first-moment values of the quadrature operators). If σ_k refers to the CM of the mode $k = c, d$, then $\Sigma_{\rm in} = \sigma_c \oplus \sigma_d$. After the evolution, characterized by the parameter $\tau \in [0, 1]$ (the BS transmissivity), the evolved CM can be written in the following block-matrix form [9,19]:

$$\Sigma_{\rm out} = \begin{pmatrix} \Sigma_1 & \Sigma_{12} \\ \Sigma_{12}^T & \Sigma_2 \end{pmatrix}, \tag{1}$$

whose elements are

$$\Sigma_1 = \tau\sigma_c + (1-\tau)\sigma_d, \tag{2a}$$

$$\Sigma_2 = \tau\sigma_d + (1-\tau)\sigma_c, \tag{2b}$$

$$\Sigma_{12} = \tau(1-\tau)(\sigma_d - \sigma_c). \tag{2c}$$

The presence of the non-zero off-diagonal terms Σ_{12} suggests the presence of correlations between the two output modes, whose amount depends on how much the incoming single mode matrix is different. It is worth noting that, if $\sigma_c = \sigma_d$, then the evolved states is uncorrelated: this effect has been theoretically [26,28] and experimentally investigated for different kind of Gaussian states [29,30]. Therefore, the correlations arise if and only if $\sigma_c \neq \sigma_d$. This can be translated into a more quantitative expression by introducing the fidelity of the two initial Gaussian states written for their covariance matrices [31]:

$$F_{cd} = \frac{1}{\sqrt{\Delta + \delta} - \sqrt{\delta}}, \tag{3}$$

where

$$\Delta = \det[\sigma_c + \sigma_d], \tag{4}$$

$$\delta = \left\{\det[\sigma_c] - \frac{1}{4}\right\}\left\{\det[\sigma_d] - \frac{1}{4}\right\}. \tag{5}$$

In [19] it has been proved that, if this quantity falls under the following threshold,

$$F_{\rm th} = \frac{4\mu_c\mu_d\sqrt{\tau(1-\tau)}}{\sqrt{g_- + 4\tau(1-\tau)g_+} - \sqrt{4\tau(1-\tau)g_-}}, \tag{6}$$

where

$$g_\pm \equiv g_\pm(\mu_c, \mu_d) = \prod_{k=c,d}(1 \pm \mu_k^2),$$

μ_k, $k = c, d$ being the purities of the two local states, then entanglement is generated, and the bipartite system emerging from the mixing is not separable. The inequality

$$F_{cd} \leq F_{\rm th} \tag{7}$$

thus represents a necessary and sufficient criterion to pre-assess entanglement resources, i.e., to assess them before they are actually employed in generation of entanglement by mixing at a beam splitter. The threshold depends on the input states' purities μ_k and on the BS transmissivity τ.

3. PROPAGATION IN NOISY CHANNELS

As a matter of fact, pure quantum states cannot be effectively produced in a laboratory. The unavoidable technical imperfections and the interaction with the environment induce decoherence on any state, which evolves into a statistical mixture, even if pure at the time of its generation. Pure quantum features, such as entanglement, are strongly affected by this mechanism; therefore, it is of fundamental interest to know how the interaction with the environment alters the parameters determining the *quantumness* of a state.

In quantum optical systems, loss of photons is a relevant source of decoherence. In addition, one may model the environment as a thermal bath made of infinite modes at thermal equilibrium and, in the most general case, each containing some residual squeezing [32–35]. In the context of an open systems approach [36], upon assuming weak coupling with the environment and the absence of any memory effect, the evolution of a single-mode propagating through a Gaussian noisy transmission channel is well described by a master equation (ME) in the Lindblad form. The ME may be then rewritten in terms of a Fokker–Planck (FP) equation for the Wigner quasi-probability distribution [3]. Because we are dealing with (zero mean) Gaussian states, the full information about the evolved state is contained in the time evolution of the CM, which reads

$$\sigma(t) = \sqrt{\mathbb{G}_t}\sigma(0)\sqrt{\mathbb{G}_t} + (\mathbb{I} - \mathbb{G}_t)\sigma_\infty, \tag{8}$$

where $\sigma(0)$ is the initial CM, $\mathbb{G}_t = e^{-\Gamma_c t}\mathbb{I} \oplus e^{-\Gamma_d t}\mathbb{I}$, Γ_k being the damping rate of mode $k = c, d$, and $\sigma_\infty = \sigma_{c,\infty} \oplus \sigma_{d,\infty}$ with

$$\sigma_{k,\infty} = \begin{pmatrix} \left(\frac{1}{2} + N_k\right) + \mathrm{Re}[M_k] & \mathrm{Im}[M_k] \\ \mathrm{Im}[M_k] & \left(\frac{1}{2} + N_k\right) - \mathrm{Re}[M_k] \end{pmatrix}, \quad (9)$$

which represents the diffusion matrix and the asymptotic CM of the system, i.e., the CM for $t \to \infty$. In Eq. (9) N_k and M_k represent the effective photon number and the squeezing parameter of the bath interacting with mode k, respectively. It is worth noting that, to ensure the positivity of the density matrix associated with the evolved state, one should have $|M_k|^2 \leq N_k(1 + N_k)$. Equation (8) suggests that the action of the lossy channel with damping rate on the CM characterizing each single system is equivalent to the action of a fictitious BS that couples each mode $k = c, d$ to the corresponding environment through its transmission coefficient $\mathbf{T}_k = e^{-\Gamma_k t}$. This simple picture does not depend on the property of the bath.

4. EXPERIMENT AND RESULTS

The *a priori* entanglement criterion discussed in Section 2 has been experimentally tested for a balanced BS, i.e., for $\tau = 1/2$ in Eq. (2). In particular, we have analyzed the mixing of pairs of squeezed modes, which are subject to different transmission channels. The two initial fields are obtained by optically manipulating the output of a frequency degenerate type-II optical parametric oscillator (OPO) working below threshold. The experimental setup [37] is based on a continuous-wave (cw) Nd:YAG laser (Innolight-Diabolo dual wavelength) internally frequency doubled. The second harmonic (532 nm) is employed as the OPO pump. The nonlinear crystal of the OPO is a 1 mm × 1.5 mm × 25 mm periodically poled α-cut KTP crystal (PPKTP) manufactured by Raicol Crystals Ltd. on custom design. The use of the α-cut PPKTP allows implementing a type II phase matching with cross-polarized signal and idler waves. The frequency-degeneracy condition, $\lambda_i = \lambda_s = 2\lambda_p = 1064$ nm (IR), is achieved at $T \sim 326$ K. The crystal temperature is actively controlled, while a Pound–Drever–Hall system [38] controls the OPO length in order to ensure pump-cavity resonance.

Our device generates an entangled bipartite Gaussian state consisting of two collinear beams (signal and idler) corresponding to two orthogonally polarized modes a and b, each excited in a thermal state [39]. Because the Hamiltonian underlying the process is $H \propto (a^\dagger b^\dagger + \mathrm{h.c.})$, which is the Hamiltonian of two-mode squeezing, by suitably manipulating the polarization of the modes a and b and letting them interfere as described in [40], it is possible to obtain two independent squeezed fields, corresponding to the states of the modes

$$c = (a + b)/\sqrt{2} \qquad d = (a - b)/\sqrt{2}.$$

In particular, the modes c and d show squeezing in orthogonal phase quadrature and, thus, represent a pair of single-mode squeezed states able to generate entanglement in a mixing process, in a scheme already exploited in the first implementation of the CV teleportation protocol [15]. Because modes c and d are, in general, *uncorrelated* squeezed states, characterized by the single-mode CMs,

$$\sigma_c = (2\mu_c)^{-1}\,\mathrm{diag}[e^{2r}, e^{-2r}], \quad (10a)$$

$$\sigma_d = (2\mu_d)^{-1}\,\mathrm{diag}[e^{-2r}, e^{2r}], \quad (10b)$$

respectively, r being the so-called squeezing parameter and μ_k the purity of mode $k = c, d$, they can be used to test the fidelity criterion. However, aiming at a more general overview of the above-mentioned criterion, we have considered different scenarios that have been investigated both theoretically and experimentally.

Experimental tests have been conducted by considering different sets of squeezed thermal states at the output of the type–II OPO (see [27,41] for details). In particular, we have selected pairs of squeezed states satisfying different conditions on their squeezing parameter and/or thermal contribution, depending on the different investigated scenarios.

A. Symmetric Passive Damping

The simplest scenario is a symmetric damping. The two uncorrelated modes undergo the same passive damping (see Fig. 1). In such a case, the evolution of the threshold and the fidelity among the two states depends on the squeezing parameter of the ancestor pure squeezed state [42]. In Fig. 2 we show the expected behavior of the threshold fidelities (solid lines) and of the actual fidelities (dashed lines) as a function of $\mathbf{T}$ (the channel transmission) for different values of the initial squeezing parameter r. Theoretical behaviors have been obtained by considering the single mode CM evolution of Eq. (8) that, in our case, reads (for the sake of simplicity we drop the subscripts c and d)

$$\sigma(\mathbf{T}) = \mathbf{T}\sigma(0) + (1 - \mathbf{T})\frac{1}{2}\mathbb{I} \quad (11)$$

$\mathbf{T} = e^{-\Gamma t}$ being the transmission coefficient and $\frac{1}{2}\mathbb{I}$ being the vacuum state CM.

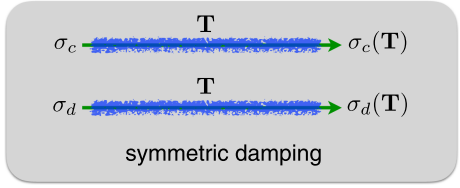

Fig. 1. Diagram of the symmetric damping channel. Modes c and d propagate through identical passive channels of transmissivity $\mathbf{T}$.

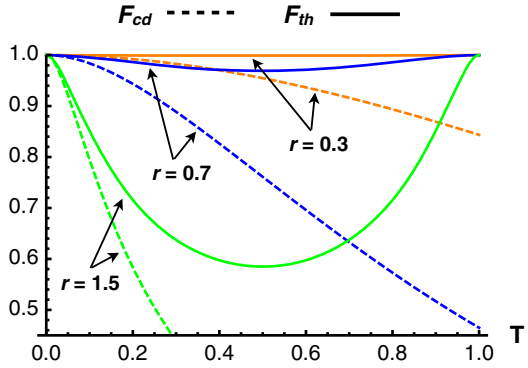

Fig. 2. Plot of the theoretical behavior of F_{cd} (dashed lines) and the corresponding threshold condition F_{th} (solid lines) at the output of two identical transmission channels as functions of transmission $\mathbf{T}$ of the channels, for three different values of initial squeezing r of the initial pure states ($\mu_c = \mu_d = 1$).

Figure 2 shows that fidelities approach 1 when the two modes are maximally attenuated ($\mathbf{T} \to 0$): in this case, as is clear from Eq. (11), they become two vacuum states; in addition, we can see that the maximum of difference between the two fidelities occurs in correspondence of fully transmitted pure states ($\mathbf{T} \to 1$). Moreover, we can see that attenuation alone is not enough to prevent initially pure squeezed states to give rise to an entangled pair because $F_{\rm th} > F_{cd}$, $\forall\, \mathbf{T} \in (0, 1]$ [27]. As we will see later, only by setting the system in contact with a thermal reservoir can we observe the violation of the entanglement condition.

In order to experimentally assess the *a priori* fidelity criterion, we have evaluated the fidelities for pairs of modes with orthogonal squeezing phases, after they had experienced the same passive damping, the noisy channel being simulated by a variable attenuator (mimicking the BS) and the characterization obtained by a homodyne detector [43]. In Fig. 3 (upper panel) we report the experimental behavior obtained for two modes undergoing the same attenuation. Experimental states have been selected from a larger set by calculating for each state the initial squeezing parameter r [44] and the actual value for the transmission $\mathbf{T}$. Then, pairs of states having the same value of r within the experimental uncertainties have been used for the plot. Contrarily to other CV separability criteria, the one investigated here depends on the states themselves. So, also the behavior of the threshold value has been experimentally verified.

In the lower panel of Fig. 3 we show a zoom of the high absorption region ($\mathbf{T} < 0.1$) to show that, by applying *a posteriori* criteria, CV entanglement can be set between very low energy states, as also verified in [43]. The plots show good agreement between the reported data and the theoretical expectation. Experimental uncertainties have been evaluated by means of the usual propagation formula. According to the theorem, if noise only springs from the photon loss, mixing two orthogonally squeezed modes in a BS always gives rise to entangled bipartite states exploitable for quantum communication tasks independently from the squeezing level [13,14].

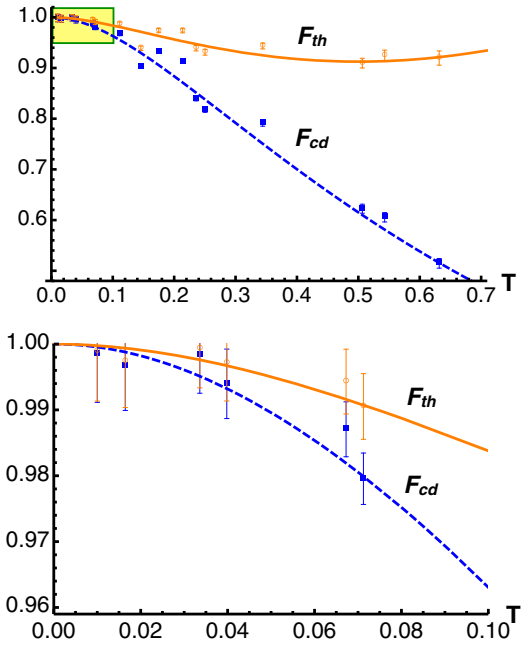

Fig. 3. Upper panel: plot of the theoretical F_{cd} (dashed line), threshold condition $F_{\rm th}$ (solid line), and corresponding experimental data (symbols) as functions of $\mathbf{T}$ when the two modes c and d pass through two identical transmission channels (see Fig. 1). Experimental data refer to pairs of states showing the same value for the squeezing parameter ($r \simeq 0.92$) of the initial pure state. Lower panel: magnification of the region highlighted in the upper-left corner of the upper panel. Experimental error bars are cropped at $F = 1.00$.

B. Symmetric Damping with Thermal Noise

Here we consider the case where one couples one of the two modes to a thermal bath with non-zero mean photon number, i.e., characterized by a non-zero effective temperature. As sketched in Fig. 4, mode c travels a Gaussian transmission channel devoid of thermal noise; thus its evolution is described by Eq. (11). Differently mode d besides attenuation is coupled to a thermal bath with a given average number of thermal photons $N_{\rm th}$. To model its evolution, we have to replace the vacuum CM in Eq. (11) by the CM corresponding to a thermal state $\sigma_\infty = (\frac{1}{2} + N_{\rm th})\mathbb{I}$, so that

$$\sigma_d(\mathbf{T}) = \mathbf{T}\sigma_d(0) + (1 - \mathbf{T})\sigma_\infty. \tag{12}$$

We stress that, in this case, the lower the transmission the higher the number of thermal photons that couple into the mode from the unused port of the BS.

The introduction of a thermal bath dramatically changes the scenario. As shown in Fig. 5, the channel may now be entanglement breaking [45], and, given the initial squeezing

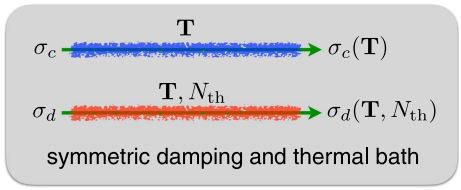

Fig. 4. Diagram of the symmetric damping channel with thermal noise. Modes c and d propagate through identical passive channels of transmissivity $\mathbf{T}$. One of the modes is also coupled to a thermal bath with $N_{\rm th} = 1.0$ average thermal photons.

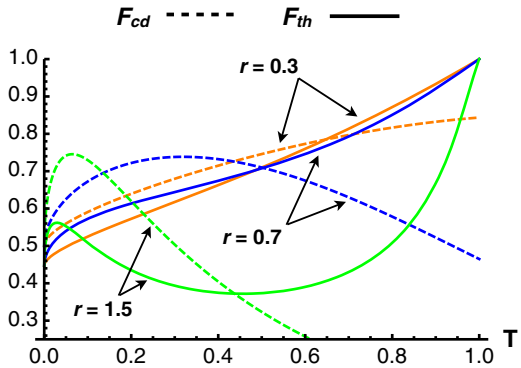

Fig. 5. Plots of F_{cd} and $F_{\rm th}$ (dashed and solid lines) as functions of $\mathbf{T}$ for different values of initial squeezing r in the presence of a thermal bath with $N_{\rm th} = 1.0$ coupled to only one of the two modes.

parameter, we find a limiting value for the transmissivity. For lower transmissivity, the thermal photons coupled to one of the modes prevent the birth of entanglement (see Fig. 5). Indeed, for each of the three squeezing parameters we have selected, we can identify a well-defined region where entanglement would not be attainable by mixing the two modes: the higher the squeezing parameter the smaller such a region.

In Fig. 6 we report the value for the critical transmission, i.e., the value $\mathbf{T}^{(c)}$ at which an intersection happens between the fidelity and the threshold as a function of r the initial squeezing parameter for a thermal bath with three different values of $N_{\rm th}$. The curves split the parameter space into two regions above the curve entanglement, where it may be obtained, whereas in the lower colored regions it cannot. As one may expect, the value of the transmission coefficient, associated with the transition, is lower for higher r, so the more the modes are squeezed the larger is the interval in which they are good as entanglement resources. We also note that, in the limit of large squeezing ($r \gg 1$), the critical transmission tends to the following asymptotic values depending only on the number of thermal photons of the bath $N_{\rm th}$:

$$\mathbf{T}^{(c)} \to 1 - \frac{\sqrt{1+N_{\rm th}(2+9N_{\rm th})} - 1 + N_{\rm th}}{2N_{\rm th}(1+2N_{\rm th})} \qquad (r \gg 1). \tag{13}$$

This sheds some light on the fundamental role of squeezing in producing entanglement by mixing two independent modes. As we have seen (Fig. 2), in the case of two pure states ($\mathbf{T} = 1$) we had $F_{\rm th} = 1$; thus any pair of even slightly different pure Gaussian states is a good entanglement resource. On the contrary the presence of thermal noise requires that at least one of the two modes is squeezed by some amount in order to produce entanglement.

The same critical transmission has been evaluated for a given squeezing parameter and a variable number of thermal photons of the bath (see Fig. 7). The increase of the thermal photons would reduce the possibility of obtaining entanglement in mixing the two modes.

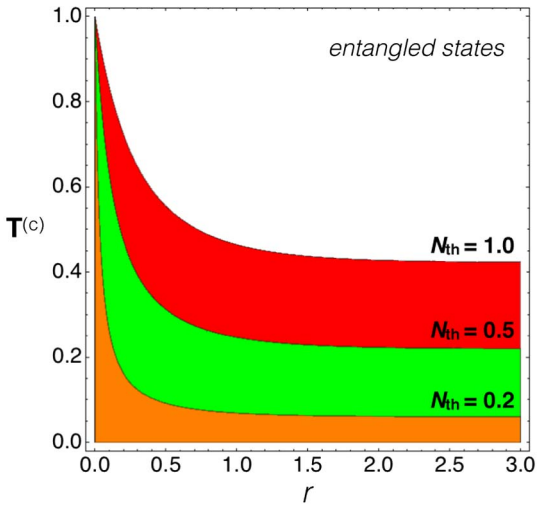

Fig. 6. Critical transmission $\mathbf{T}^{(c)}$ as a function of r for different values of $N_{\rm th}$ (from top to bottom $N_{\rm th} = 1.0$, 0.5, and 0.2). Colored regions below the curves show where entanglement cannot be achieved, whereas above the curves one obtains always an entangled output state.

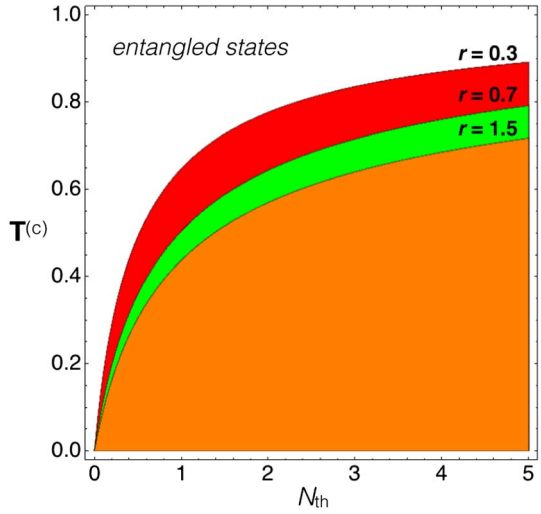

Fig. 7. Critical transmission $\mathbf{T}^{(c)}$ as a function of $N_{\rm th}$, the average thermal photon number of the bath, for different values of the squeezing parameter, from top to bottom $r = 0.5$, 0.7, and 1.5. Curves divide the parameter plane into two regions: above the lines entanglement can be achieved, below (colored regions) it cannot.

C. Asymmetric Damping

In entanglement distribution schemes [46–49] it may happen that the channels have different transmissivities. In our case, this means that the two squeezed fields arrive at the mixing BS after having suffered different attenuations. This situation is sketched in Fig. 8, where we assume that mode d travels along a channel with a transmission $0.9\mathbf{T}$, if $\mathbf{T}$ is the value corresponding to mode c.

The effects of such an asymmetry can be seen in Fig. 9. It is evident that the transmission asymmetry does not play any effective role in corrupting the two states' properties. Compared with the symmetric case discussed in Fig. 2, the only clear difference can be found in the threshold fidelity $F_{\rm th}$ for modes affected by lower losses ($\mathbf{T} \gtrsim 0.9$): mode c purity is close to 1, while mode d has already suffered an effective decoherence.

This effect can be more clearly understood considering a scenario in which one of the two modes stays pure, while the other mode experiences a passive channel of transmission $\mathbf{T}$ (as sketched in Fig. 10). The results, shown in Fig. 11, prove

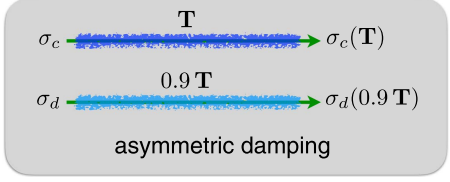

Fig. 8. Diagram of the asymmetric damping channel. Modes c and d propagate through two channels of different transmissivity. In particular, for any value of $\mathbf{T}$ we assume that mode c is transmitted through a channel with transmission $\mathbf{T}$, whereas mode d propagates through a channel with transmission $0.9\mathbf{T}$.

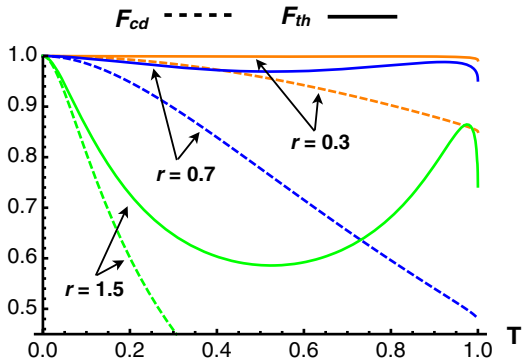

Fig. 9. Plot of the theoretical behavior of F_{cd} and $F_{\rm th}$ (dashed and solid lines, respectively) as functions of $\mathbf{T}$ for different values of the initial squeezing r. Modes c and d propagate through different channels with transmissivities $\mathbf{T}$ and $0.9\mathbf{T}$, respectively.

once more that the two modes outing a balanced BS illuminated by a single squeezed field (with the vacuum entering through its unused port) are entangled. As shown in Fig. 11 for any value of initial squeezing at $\mathbf{T} = 0$ (namely, mode d is in the vacuum state) we have $F_{cd} < F_{\rm th}$. This scenario also has been investigated experimentally. We have addressed the fidelity among a single pure ancestor state, retrieved from the experiment, and the whole set of the mixed states corresponding to the same pure ancestor but for different effective channel transmissions. The experimental curve has been obtained by selecting, among the measured CMs, all those corresponding to the transmission of a pure squeezed state with $r = 0.57$

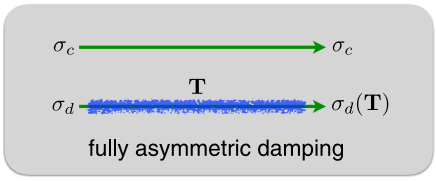

Fig. 10. Diagram of the fully asymmetric damping channel. Mode c propagates in an ideal lossless channel (and stays pure), whereas mode d travels a passive transmission channel with transmission coefficient $\mathbf{T}$.

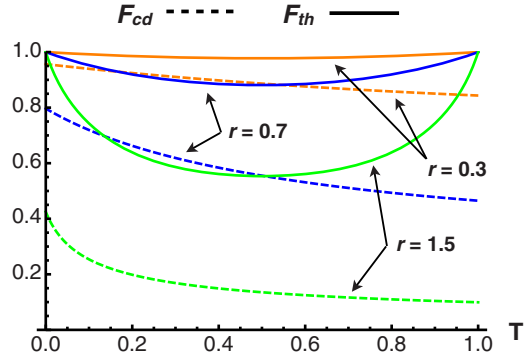

Fig. 11. Plot of the theoretical behavior of F_{cd} (dashed line) and $F_{\rm th}$ (solid line) as functions of $\mathbf{T}$ and different values of the initial squeezing r for the fully asymmetric damping scheme of Fig. 10.

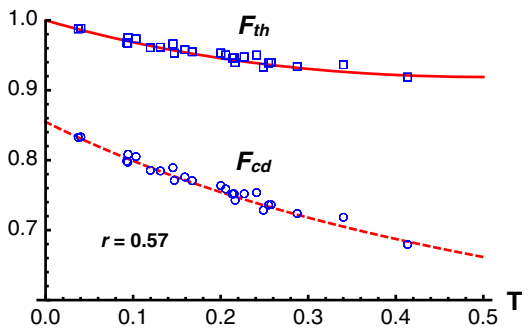

Fig. 12. Plot of the theoretical (lines) and experimental (squares and circles) fidelity F_{cd} (dashed line) and the threshold condition (solid line) as functions of $\mathbf{T}$, when one of the two modes remains pure, while the other travels a passive transmission channel (see Fig. 10). Experimental data refer to a set of measured CMs showing the same value of the squeezing parameter ($r = 0.57$) for the ancestor pure state.

(within experimental uncertainty). The corresponding plot is reported, together with the corresponding theoretical curve, in Fig. 12: even at very low transmission the measured fidelity is well below the threshold value, revealing the generation of entanglement at the output of a balanced BS illuminated by a single mode squeezed field.

D. Asymmetric Damping with Thermal Noise

The last case we have investigated is the situation where asymmetric damping is associated with thermal noise affecting one of the squeezed modes (see Fig. 13). The expected behavior of the fidelities is reported in Fig. 14. In this case the left end of the plot (i.e., for $\mathbf{T} \to 0$) corresponds to mixing one squeezed mode to a thermal state with an average photon number $N_{\rm th} = 1.0$. Upon comparing the plot in Fig. 14 to that of Fig. 11, one may appreciate the effect of adding a thermal bath, i.e., coupling thermal photons to a squeezed field. In this case, both the value of the threshold and the fidelity between the two modes decrease with $\mathbf{T}$. In particular, for small values of the initial squeezing (e.g., $r = 0.3$) the overall effect of the thermal contribution is to prevent entanglement generation.

We have experimentally investigated the role of thermal photons coupled to one of the squeezed modes by selecting reconstructed states with the same measured value of squeezing r (i.e., the residual squeezing parameter of the state after the transmission) but different thermal contents. We note that, experimentally, this amounts to considering states coming from different pure ancestors and undergoing different levels of

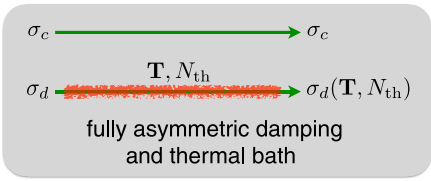

Fig. 13. Diagram of the fully asymmetric damping channel. Compared with the scheme of Fig. 10 now mode d is also coupled to a thermal bath.

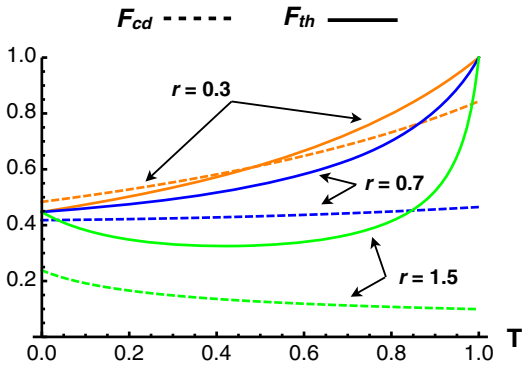

Fig. 14. Plot of F_{cd} (dashed lines) and the threshold $F_{\rm th}$ (solid lines) as functions of **T** for the scheme of Fig. 13. We consider three different values of the initial squeezing r. Mode c is prepared in a pure squeezed state, whereas mode d travels through a damping channel, also coupled to a bath having $N_{\rm th} = 1.0$ average thermal photons.

transmission. In this way for the same residual squeezing ($r = 0.26$ in Fig. 15) the effective average number of thermal photon is different. In the upper panel of Fig. 15 we show the fidelity F_{cd}, compared with the corresponding threshold $F_{\rm th}$, as functions of thermal photons $N_{\rm th}$ effectively coupled into mode d. Actually, these thermal photons are obtained by letting mode d propagate in a lossy channel. In fact, in such a case, it is well known that a squeezed field transforms into a squeezed thermal state [44]. The results, as reported in Fig. 15, show that the distance to the threshold decreases as the thermal contribution increases. This behavior may be seen more clearly in the lower panel of the same figure, where we show the difference between the two fidelities.

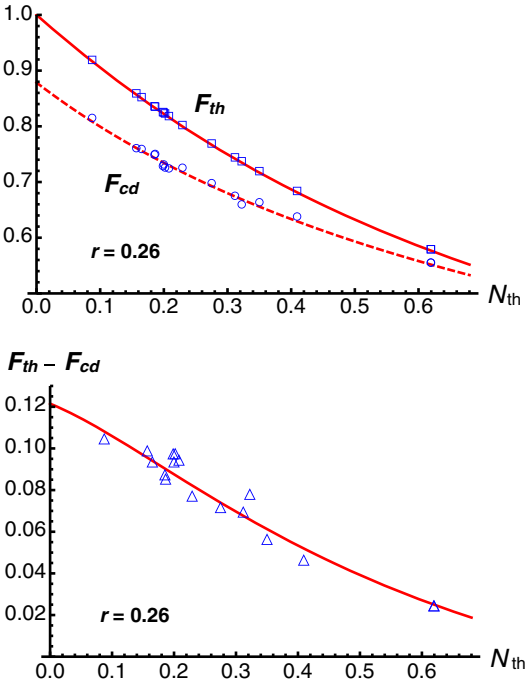

Fig. 15. Upper panel: theoretical threshold fidelity $F_{\rm th}$ (solid) and actual fidelity F_{cd} (dashed) together with the corresponding experimental data (open squares and open circles, respectively) as a function of the average number of bath thermal photons $N_{\rm th}$ for the scheme sketched in Fig. 13. Experimental data correspond to a set of states with the same value of the squeezing parameter ($r = 0.26$) after the transmission. Lower panel: plot of the difference between $F_{\rm th}$ and F_{cd} (those shown in the upper panel) together with the corresponding experimental data.

5. CONCLUSIONS

We have experimentally implemented an *a priori* certification scheme based on the fidelity criterion for entanglement generation and exploited our scheme to assess the effects of losses and noise on the generation of entanglement by Gaussian states mixing. In particular, we have analyzed the effect of signal propagation before the BS and evaluated threshold values on the transmission coefficient and on the thermal noise as a function of the parameters of the input signals. We have considered both symmetric and asymmetric channels with and without thermal noise.

Our results show that the fidelity criterion represents a reliable tool for entanglement certification and allows us to accurately take into account the imperfections of the generation scheme, including asymmetries and background noise. More generally, our results allow one to pre-assess entanglement resources and to optimize the design of BS-based schemes for the generation of entanglement for continuous variable quantum technology.

Funding. Università degli Studi di Milano (H2020 Transition 15-6-3008000-625).

Acknowledgment. S. O. and M. G. A. P. thank the late Rodolfo Bonifacio for his vigorous teaching in the field of quantum optics.

REFERENCES

1. S. L. Braunstein and P. van Loock, "Quantum information with continuous variables," Rev. Mod. Phys. **77**, 513–577 (2005).
2. C. Weedbrook, S. Pirandola, R. García-Patrón, N. J. Cerf, T. C. Ralph, J. H. Shapiro, and S. Lloyd, "Gaussian quantum information," Rev. Mod. Phys. **84**, 621–669 (2012).
3. A. Ferraro, S. Olivares, and M. G. A. Paris, *Gaussian States in Quantum Information* (Bibliopolis, 2005).
4. J. Eisert and M. B. Plenio, "Introduction to the basics of entanglement theory in continuous-variable systems," Int. J. Quantum Inf. **1**, 479–506 (2003).
5. F. Dell'Anno, S. De Siena, and F. Illuminati, "Multiphoton quantum optics and quantum state engineering," Phys. Rep. **428**, 53–168 (2006).
6. X.-B. Wang, T. Hiroshima, A. Tomita, and M. Hayashi, "Quantum information with Gaussian states," Phys. Rep. **448**, 1–111 (2007).
7. G. Adesso and F. Illuminati, "Entanglement in continuous-variable systems: recent advances and current perspectives," J. Phys. A **40**, 7821–7880 (2007).
8. M. M. Wolf, G. Giedke, and J. I. Cirac, "Extremality of Gaussian quantum states," Phys. Rev. Lett. **96**, 080502 (2006).
9. S. Olivares, "Quantum optics in the phase space," Eur. Phys. J. **203**, 3–24 (2012).
10. C. T. Lee, "Nonclassical photon statistics of two-mode squeezed states," Phys. Rev. A **42**, 1608–1616 (1990).
11. C. T. Lee, "Measure of the nonclassicality of nonclassical states," Phys. Rev. A **44**, R2775–R2778 (1991).

12. C. T. Lee, "Moments of *P* functions and nonclassical depths of quantum states," Phys. Rev. A **45**, 6586–6595 (1992); Erratum Phys. Rev. A 49, 45 (1994).
13. M. S. Kim, W. Son, V. Buzek, and P. L. Knight, "Entanglement by a beam splitter: nonclassicality as a prerequisite for entanglement," Phys. Rev. A **65**, 032323 (2002).
14. X.-B. Wang, "Theorem for the beam-splitter entangler," Phys. Rev. A **66**, 024303 (2002).
15. A. Furusawa, J. L. Sørensen, S. L. Braunstein, C. A. Fuchs, H. J. Kimble, and E. S. Polzik, "Unconditional quantum teleportation," Science **282**, 706–709 (1998).
16. G. Masada, K. Miyata, A. Politi, T. Hashimoto, J. L. O'Brien, and A. Furusawa, "Continuous-variable entanglement on a chip," Nat. Photonics **9**, 316–319 (2015).
17. V. D'Auria, S. Fornaro, A. Porzio, S. Solimeno, S. Olivares, and M. G. A. Paris, "Full characterization of bipartite entangled states by a single homodyne detector," Phys. Rev. Lett. **102**, 020502 (2009).
18. S. Cialdi, C. Porto, D. Cipriani, S. Olivares, and M. G. A. Paris, "Full quantum state reconstruction of symmetric two-mode squeezed thermal states via spectral homodyne detection and a state-balancing detector," Phys. Rev. A **93**, 043805 (2016).
19. S. Olivares and M. G. A. Paris, "Fidelity matters: the birth of entanglement in the mixing of Gaussian states," Phys. Rev. Lett. **107**, 170505 (2011).
20. A. Peres, "Separability criterion for density matrices," Phys. Rev. Lett. **77**, 1413–1415 (1996).
21. P. Horodecki, "Separability criterion and inseparable mixed states with positive partial transposition," Phys. Lett. A **232**, 333–339 (1997).
22. R. Simon, "Peres-Horodecki separability criterion for continuous variable systems," Phys. Rev. Lett. **84**, 2726–2729 (2000).
23. L.-M. Duan, G. Giedke, J. I. Cirac, and P. Zoller, "Inseparability criterion for continuous variable systems," Phys. Rev. Lett. **84**, 2722–2725 (2000).
24. M. D. Reid, "Demonstration of the Einstein-Podolsky-Rosen paradox using nondegenerate parametric amplification," Phys. Rev. A **40**, 913–923 (1989).
25. I. I. Arkhipov, J. Perina, Jr., J. Perina, and A. Miranowicz, "Interplay of nonclassicality and entanglement of two-mode Gaussian fields generated in optical parametric processes," Phys. Rev. A **94**, 013807 (2016).
26. S. Olivares, "Interference of multi-mode Gaussian states and non-appearance of quantum correlations," Int. J. Quantum Inf. **10**, 1241004 (2012).
27. D. Buono, G. Nocerino, A. Porzio, and S. Solimeno, "Experimental analysis of decoherence in continuous-variable bipartite systems," Phys. Rev. A **86**, 042308 (2012).
28. S. Olivares and M. G. A. Paris, "Entanglement-induced invariance in bilinear interactions," Phys. Rev. A **80**, 032329 (2009).
29. R. Bloomer, M. Pysher, and O. Pfister, "Nonlocal restoration of two-mode squeezing in the presence of strong optical loss," New J. Phys. **13**, 063014 (2011).
30. A. Meda, S. Olivares, I. P. Degiovanni, G. Brida, M. Genovese, and M. G. A. Paris, "Revealing interference by continuous variable discordant states," Opt. Lett. **38**, 3099–3102 (2013).
31. H. Scutaru, "Fidelity for displaced squeezed thermal states and the oscillator semigroup," J. Phys. A **31**, 3659–3663 (1998).
32. T. A. B. Kennedy and D. F. Walls, "Squeezed quantum fluctuations and macroscopic quantum coherence," Phys. Rev. A **37**, 152–157 (1988).
33. P. Tombesi and D. Vitali, "Physical realization of an environment with squeezed quantum fluctuations via quantum-nondemolition-mediated feedback," Phys. Rev. A **50**, 4253–4257 (1994).
34. N. Lütkenhaus, J. I. Cirac, and P. Zoller, "Mimicking a squeezed-bath interaction: quantum-reservoir engineering with atoms," Phys. Rev. A **57**, 548–558 (1998).
35. A. R. Rossi, S. Olivares, and M. G. A. Paris, "Degradation of continuous variable entanglement in a phase-sensitive environment," J. Mod. Opt. **51**, 1057–1061 (2004).
36. H.-P. Breur and F. Petruccione, *The Theory of Open Quantum Systems* (Oxford University, 2002).
37. V. D'Auria, S. Fornaro, A. Porzio, E. A. Sete, and S. Solimeno, "Fine tuning of a triply resonant OPO for generating frequency degenerate CV entangled beams at low pump powers," Appl. Phys. B **91**, 309–314 (2008).
38. R. W. P. Drever, J. L. Hall, F. V. Kowalski, J. Hough, G. M. Ford, A. J. Munley, and H. Ward, "Laser phase and frequency stabilization using an optical resonator," Appl. Phys. B **31**, 97–105 (1983).
39. A. Porzio, V. D'Auria, S. Solimeno, S. Olivares, and M. G. A. Paris, "Homodyne characterization of continuous variable bipartite states," Int. J. Quantum Inf. **5**, 63–68 (2007).
40. V. D'Auria, A. Porzio, S. Solimeno, S. Olivares, and M. G. A. Paris, "Characterization of bipartite states using a single homodyne detector," J. Opt. B **7**, S750–S753 (2005).
41. D. Buono, G. Nocerino, V. D'Auria, A. Porzio, S. Olivares, and M. G. A. Paris, "Quantum characterization of bipartite Gaussian states," J. Opt. Soc. Am. B **27**, A110–A118 (2010).
42. D. Buono, G. Nocerino, S. Solimeno, and A. Porzio, "Different operational meanings of continuous variable Gaussian entanglement criteria and Bell inequalities," Laser Phys. **24**, 074008 (2014).
43. G. Nocerino, D. Buono, A. Porzio, and S. Solimeno, "Survival of continuous variable entanglement over long distances," Phys. Scr. **T153**, 014049 (2013).
44. V. D'Auria, C. de Lisio, A. Porzio, S. Solimeno, and M. G. A. Paris, "Transmittivity measurements by means of squeezed vacuum light," J. Phys. B **39**, 1187–1198 (2006).
45. A. De Pasquale, A. Mari, A. Porzio, and V. Giovannetti, "Amendable Gaussian channels: restoring entanglement via a unitary filter," Phys. Rev. A **87**, 062307 (2013).
46. N. Hosseinidehaj and R. Malaney, "Gaussian entanglement distribution via satellite," Phys. Rev. A **91**, 022304 (2015).
47. L. Praxmeyer and P. van Loock, "Near-unit-fidelity entanglement distribution scheme using Gaussian communication," Phys. Rev. A **81**, 060303(R) (2010).
48. A. Ferraro, M. G. A. Paris, A. Allevi, A. Andreoni, M. Bondani, and E. Puddu, "Three-mode entanglement by interlinked nonlinear interactions in optical $\chi^{(2)}$ media," J. Opt. Soc. Am. B **21**, 1241–1249 (2004).
49. M. Bondani, A. Allevi, A. Andreoni, E. Puddu, A. Ferraro, and M. G. A. Paris, "Properties of two interlinked $\chi^{(2)}$ interactions in non-collinear phase-matching," Opt. Lett. **29**, 180–182 (2004).